Polymer Chemistry

RAFT Polymerization of an Aromatic Organoborane for Block Copolymer Synthesis

Journal:	*Polymer Chemistry*
Manuscript ID	PY-ART-06-2023-000706.R1
Article Type:	Paper
Date Submitted by the Author:	18-Aug-2023
Complete List of Authors:	Melvin, Sophia; Johns Hopkins University, Chemistry Mediavilla, Braden; Johns Hopkins University Ambrosius, Em; Johns Hopkins University Jiang, Qifeng; Johns Hopkins University - Homewood Campus, Fang, Fan; Johns Hopkins University Ji, Yuyang; Johns Hopkins University Mukhopadhaya, Tushita; Johns Hopkins University, Materials Science and Engineering; Johns Hopkins University Katz, Howard; Johns Hopkins University, Materials Science and Engineering Klausen, Rebekka; Johns Hopkins University, Chemistry

RAFT Polymerization of an Aromatic Organoborane for Block Copolymer Synthesis

Sophia J. Melvin,[a] Braden A. Mediavilla,[a] Em G. Ambrosius,[a] Qifeng Jiang,[a] Fan Fang,[a] Yuyang Ji,[a] Tushita Mukhopadhyaya[b], Howard E. Katz[b] and Rebekka S. Klausen [a*]

[a] Department of Chemistry, Johns Hopkins University, 3400 N. Charles St, Baltimore, MD, USA 21218
[b] Department of Materials Science and Engineering, Johns Hopkins University, 3400 N. Charles St, Baltimore, MD, USA 21218
‡ Present address: Department of Chemistry, Columbia University, 3000 Broadway, New York, NY, US 10027
* klausen@jhu.edu

Abstract

Synthesizing polystyrene-*block*-poly(vinyl alcohol) (PS-*b*-PVA) via controlled radical polymerization of vinyl acetate, the traditional precursor to polyvinyl alcohol (PVA), is challenging due to the reactivity of the unconjugated α-acetoxy radical. We report the synthesis and characterization of PS-*b*-PVA block copolymers (BCPs) with tailorable PVA block lengths via RAFT polymerization of an alternative precursor, an aromatic organoborane comonomer BN 2-vinylnapthalene (BN2VN). RAFT homopolymerization of BN2VN (RB) using 2-cyano-2-propyl dodecyl trithiocarbonate (CPDT) is described. Solid-state NMR, ATR-IR, SEC and thermogravimetric analysis reveal significant differences between PS-*b*-PVA and RS-*b*-RB. The fate of the trithiocarbonate end-group during oxidative conversion of the C–B side chain to a C–OH side chain was studied; while a hydrated aldehyde (e.g., gem-diol) was hypothesized, conclusive evidence was not found.

Introduction

Herein, we report radical addition-fragmentation chain transfer polymerization of BN 2-vinylnaphthalene (BN2VN), an aromatic monomer with a transformable side chain, that affords access to the amphiphilic copolymer polystyrene-*block*-polyvinyl alcohol (PS-*b*-PVA).

Vinyl acetate (VAc), the traditional precursor to PVA via radical polymerization and side chain deprotection,[1] has historically been a challenging monomer for controlled radical polymerization (CRP) methodologies such as atom-transfer radical polymerization (ATRP),[2] nitroxide-mediated polymerization (NMP),[3] and reversible addition-fragmentation chain transfer (RAFT)[4] polymerization. The intermediate α-acetoxy radical is not as stabilized as the radicals derived from more activated monomers (MAMs, e.g., styrene (St)), resulting in higher rates of undesired chain-transfer pathways.[5–8]

These challenges inspired deep investigation of VAc polymerization and there have been several reports achieving PVAc with M_w/M_n < 1.5. In 1994 the first controlled polymerization of PVAc was reported by Mardare and Matyjaszewski using an aluminum complex formed from a trialkylaluminum and 2,2,6,6-tetramethyl-l-piperidinyloxy (TEMPO), although deprotection to PVA was not described.[9] Additional examples include NMP, alkyl halide degenerative transfer, metal complex-mediated radical polymerization

(utilizing cobalt, vanadium, or iron), ATRP, and MADIX/RAFT.[9–17] Xanthate chain transfer agents are particularly effective for VAc controlled radical polymerization.[12]

The differences between VAc and St CRP also limit synthetic access to diblock copolymers (BCPs) that include the hydrophilic vinyl alcohol (VA) block and the hydrophobic PS block (PS-*b*-PVA), as the methodologies optimized for VAc homopolymerization may not always be effective for MAMs like styrene. Well-defined PS-*b*-PVA would be notable because of the keen interest in high χ-low N BCPs for lithography,[18] where the greater the difference in polarity (χ) between two blocks, the lower the degree of polymerization (N) needed for phase separation. For example, Youk et al. reported that cobalt-mediated radical polymerization (CMRP) accessed well-defined PVAc capped with a $Co(acac)_2$ end group; addition of St afforded PVAc-*b*-PS with an average St block length of 2 units.[19] PVAc BCP synthesis has often been accomplished with two successive methodologies (CMRP-RAFT,[19] CMRP-ATRP,[20,21] and ATRP-RAFT[22]) via end group functionalization or macromolecular click reactions.[23] Examples of a single methodology include a bifunctional iniferter facilitating successive RAFT VAc polymerization and St ATRP.[24] Zhu et al. reported a single dithiocarbamate, nonhydrolyzable iniferter for both VAc and St polymerization.[25] Sequential cationic polymerization of St and a vinyl ether, followed by ether deprotection, avoids VAc.[26]

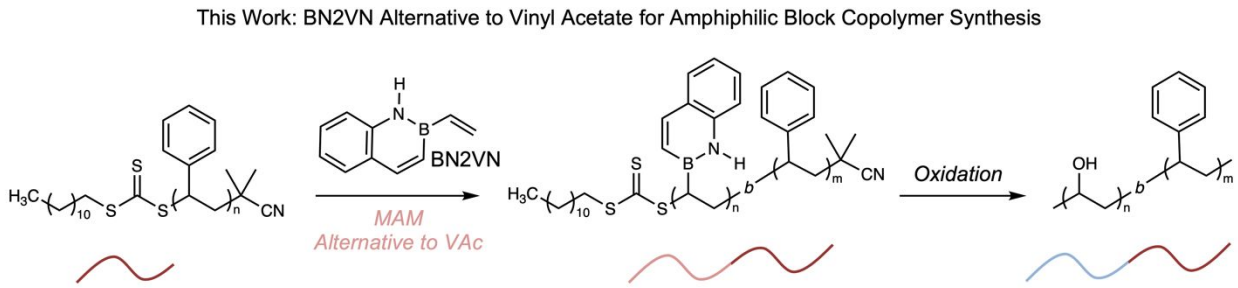

Scheme 1. This work: BN2VN, a more activated monomer (MAM), as an alternative to vinyl acetate (VAc) for the synthesis of vinyl alcohol block copolymers.

We considered if an alternative monomer to VAc might not only access PS-*b*-PVA, but also in the long-term enable new opportunities (Scheme 1). In prior work, we reported the aromatic organoborane BN2VN as an alternative to VAc for the synthesis of VA (co)polymers by either free radical[27–31] or coordination polymerization.[32,33] We showed that BN2VN exhibited a closer match to styrene in terms of reactivity ratios than either VAc or vinyl siloxanes, which was attributed to the aromatic nature of the BN naphthalene side chain.[30,34] Therefore, BN2VN might be suitable for the synthesis of PS-*b*-PVA via a single methodology, while having the advantage that the PBN2VN to PVA transformation can occur under either aqueous[27] or organic[29] oxidative conditions, which could result in greater range of functionalized comonomers beyond styrene. Organoboranes are versatile intermediates in organic synthesis, capable of transformation to C–C,[35] C–halide, and C–N bonds,[36] and PBN2VN blocks may have potential for conversion to other side chains. Nishikawa and Ouchi reported the free and controlled radical polymerization of isopropenyl pinacol boronate ester (IPBpin) and transformation to both poly(methylvinyl alcohol) and poly(methylvinyl amine).[37,38]

Herein we report an initial study of BN2VN suitability for RAFT polymerization, as well as transformation to PVA. We found that the addition of 2-cyano-2-propyl dodecyl trithiocarbonate (CPDT), a styrenic RAFT agent, to BN2VN homopolymerization afforded

PBN2VN with "living" characteristics (e.g., M_w/M_n <1.5) at low conversion. At higher conversions, erosion in control was observed. Thermogravimetric analysis (TGA) provided evidence of the trithiocarbonate (TTC) end group. We also investigated the preparation of PBN2VN-*b*-PS via either St polymerization from CPDT-PBN2VN or via BN2VN polymerization from CPDT-PS. Finally, we showed that C–B to C–OH interconversion was successful, providing PVA-*b*-PS. End group analysis suggested that the TTC was hydrolytically cleaved, forming a hydrated aldehyde or gem-diol.

Experimental

Synthesis of RB: RAFT Polymerization of BN2VN. In a glovebox, a rare earth stir bar was added to a 10 mL thick-walled vessel, followed by BN2VN (3.22 mmol, 0.500 g). Via microsyringe, CPDT (0.033 mmol, 23 μL) stock solution in THF (1.4 M) was added to the vessel. AIBN stock solution in THF (0.39 M) was added to the vessel (0.029 mmol, 75 uL). The vessel was sealed, removed from the glovebox, and submerged in a 60 °C preheated oil bath. After completion, the reaction was stopped by submerging the vessel in a dewar with liquid nitrogen then uncapped and opened to air. Product was dissolved in minimal DCM (5 mL) and precipitated in MeOH (50 mL) and isolated via vacuum filtration with a fritted funnel. The precipitation and filtration process was repeated three times. The final product was dried in a vacuum oven overnight at 60 °C before characterization.

Synthesis of RS: RAFT Polymerization of Styrene. The large-scale bulk polymerization was performed in a glovebox. To a 100 mL Schlenk flask was added a large rare earth stir bar and filtered inhibitor-free styrene (0.2 mol, 20.83 g). CPDT was weighed out and added to the vessel (0.002 mol, 0.691 g). AIBN was added to the vessel (0.0002 mol, 32.8 mg). The flask was sealed with an adapter and septum, removed from the glovebox, attached to a Schlenk line and opened to argon then submerged stirring in a 70 °C preheated oil bath. After completion, the reaction was stopped by submerging the vessel in a dewar with liquid nitrogen then uncapped and opened to air. Product was dissolved in rounds of DCM (5 mL) until viscous but pipette-able and precipitated in MeOH (50 mL) until and isolated via filtration. The precipitation and filtration process was repeated three times. The final product was dried in a vacuum oven overnight at 60 °C before characterization.

Attempted Synthesis of RS-*b*-RB: Chain Extension of RB with Styrene. In a glovebox, CPDT-PBN2VN (100 mg) was added to a thick-walled 10 mL vessel. Filtered inhibitor-free styrene (0.67 mmol, 69.8 mg) was added to the vessel. An AIBN stock solution (0.1 mL, 0.67uM) in THF (1.1 mM) was added to the vessel via syringe. The vessel was then sealed, removed from the glovebox, and submerged in a 70 °C preheated oil bath. After completion, the reaction was stopped by submerging the vessel in a dewar with liquid nitrogen then uncapped and opened to air. Product was dissolved in minimal DCM (3 mL) and precipitated in MeOH (30 mL), isolated via filtration. The precipitation and filtration process was repeated three times. The final product was dried in a vacuum oven overnight at 60 °C before characterization.

Synthesis of RS-*b*-RB: Chain Extension of RS with BN2VN. For 1:1 mass feed ratio, in a glovebox of CPDT-PS (0.5 g) and BN2VN (3.22 mmol, 0.5 g) were crushed and combined with mortar and pestle into a homogenous powder, then added to a thick-walled 10 mL vessel with a rare-earth stir bar. AIBN stock solution in THF (0.029 mmol, 75 uL of 0.39 M) was added to the vessel. The vessel was sealed, removed from the glovebox and submerged in a preheated 60 °C oil bath. After completion, the reaction was stopped by submerging the vessel in a dewar with liquid nitrogen then uncapped and opened to air. Product was dissolved in minimal DCM (5 mL) and precipitated in MeOH (50 mL), and isolated via filtration. The precipitation and filtration process was repeated three times. The final product was dried in a vacuum oven overnight at 60 °C before characterization.

Synthesis of PS-*b*-PVA: Oxidation of RS-*b*-RB. In a 200 mL round bottom equipped with a stir bar was added 200 mg block copolymer RS-*b*-RB, 5 mL of 6M NaOH, 25 mL THF, and 5 mL ethanol. Once stirring, 10 mL of 30% H_2O_2 was added dropwise with a glass pipette. A condenser was added and the reaction was left to stir open to air for 30 minutes before heating to 65 °C and run overnight with a yellow tapered flange plug. The reaction was cooled to room temperature and quenched with 6M HCl until neutralized (approx. 4 mL). Organic solvents were removed in vacuo and solid product was isolated via filtration, rinsing with water. Attempts to remove residual boric acid byproducts were conducted with three repeats of dissolving material in 5 mL methanol and rotovapping at 40 °C. Isolated product was dried in a vacuum oven overnight at 60 °C.

Thermal gravimetric analysis (TGA). Thermogravimetric analysis (TGA) curves were collected with samples (~ 20 mg) in a pan heated from room temperature to 600 °C under N_2 atmosphere at a heating rate of 3 °C/min and N_2 flow rate of 100 mL/min.

Molecular weight analysis by size exclusion chromatography (SEC). Polymer molecular weights were measured by gel permeation chromatography (GPC) and multi-angle light scattering (MALS) on a Tosoh Bioscience EcoSEC GPC workstation using butylated hydroxytoluene stabilized tetrahydrofuran (THF) as the eluent (0.35 mL min^{-1}, 40 °C) through TSKgel SuperMultipore HZ-M guard column (4.6 mm ID x 2.0 cm, 4 µm, Tosoh Bioscience) and a TSKgel SuperMultipore HZ-M column (4.6 mm ID x 15 cm, 4 µm, Tosoh Bioscience) and Tosoh LenS3 MALS Detector (0.35 mL min^{-1}, 20 Hz Acquisition Rate). Polystyrene standards (EasiVial PS-M, Agilent) were used to build a calibration curve. Processing was performed using EcoSEC Data Analysis software (Version 1.14, Tosoh Bioscience) and SECview software (Version 1.0.1224, Tosoh Bioscience). Polymers were dissolved in THF (1 mg mL^{-1}), filtered (Millex-FG Syringe Filter Unit, 0.20 µm, PTFE, EMD Millipore), and injected using an auto-sampler (10 µL). In order to report the most accurate molecular weight characteristics, we took M_w values from light scattering SEC modes ($M_{w,MALS}$), dispersity values from conventional analysis SEC modes ($M_w/M_{n,\ RI}$), and a calculated M_n from those values ($M_{n,CALC}$). M_w values determined via conventional calibration is relative to a standard and not a reflection of true M_w, M_w values determined from light scattering modes in MALS are absolute and independent of retention time shift so long as the input concentration remains exact. But because scattered light intensity is proportional to M_w, the higher the M_w the higher the intensity and vice versa, it is not a real reflection of concentration distribution between short and long chain species. As a result, MALS light scattering modes typically underestimates dispersity giving narrower-than-real values whereas conventional calibration more accurately predicts dispersity values. We used this method in our conversion study analyses and otherwise report values from both methods.

Results and Discussion

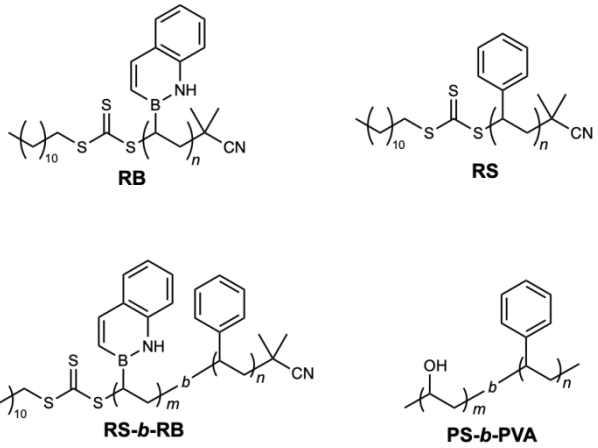

Chart 1. Chemical structures of macromolecules synthesized herein.

RAFT Polymerization of BN2VN.

A wide range of chain transfer agents (CTAs) have been reported in which modification of the thiocarbonyl structure tailors chain transfer reactivity to match monomer characteristics. Trithiocarbonates like 2-cyano-2-propyl dodecyltrithiocrbonate (CPDT) are well-suited to more activated monomers like styrene, while thiocarbamates[25] or xanthates[23] are typically matched to less activated monomers like VAc. Therefore, the identity of an appropriate CTA is evidence for the reactivity character of a given monomer.

We chose to investigate CPDT for BN2VN RAFT polymerization due to evidence of its suitability for conjugated monomers and boron-based monomers. Nishikawa and Ouchi previously investigated suitable CTAs for RAFT polymerization of IPBpin and found that CPDT provided effective molecular weight control (e.g., $M_w/M_n < 1.2$) and reasonable reaction rates at a IPBpin:CPDT:AIBN ratio of 100:1.0:0.9.[38] While this ratio of reagents is atypical, the ratio of CTA:initiatior is typically closer to 100:1, they reported that higher reaction rates were possible with more initiator present. To facilitate direct comparison of the two vinylboranes, we have also employed this same ratio of BN2VN:CPDT:AIBN of 100:1.0:0.9. Results using a more typical, lower proportion of AIBN are reported in Figure S1. As seen for IPBpin, we also observed shorter reaction times and higher conversions with more initiator.

Chart 1 summarizes the chemical structures of macromolecules synthesized by RAFT polymerization discussed in this manuscript. We determined the evolution of molecular weight characteristics of **RB** over time. Molecular weight characteristics were determined by size exclusion chromatography relative to polystyrene standards (stabilized THF, 1 mg/mL, RT), as well as by multi-angle light scattering (MALS) (Table 1). We elected to report both data sets because while RB closely resembles polystyrene, the calibration standard, oxidation to PVA would drastically change solubility characteristics and introduce the potential for self-assembly, which would be expected to result in anomalous molecular weight characteristics using SEC. Styrene and BN2VN polymers (e.g., $\mathbf{RB_{36}}$) are named after the number-average degree of polymerization as estimated from MALS data (see Methods section). Vinyl alcohol BCP's derived from BN2VN BCP's are named according to the degree of polymerization of the starting block.

Conversion was determined gravimetrically. Estimation of conversion by ^{1}H NMR was not possible due to the broadness of the PBN2VN peaks, which overlapped any residual monomer peaks or internal standard. After 9 h, 51.1% conversion was reached. This is slightly faster than the more hindered IPBpin, with a half-life closer to 12 hours.[38] Time-conversion data for vinylboronic pinacol ester (VBpin) RAFT homopolymerization have not been described, but reaction times in excess of 72 hours have been described for copolymerization with styrene, suggesting a comparatively slow rate of polymerization.[39]

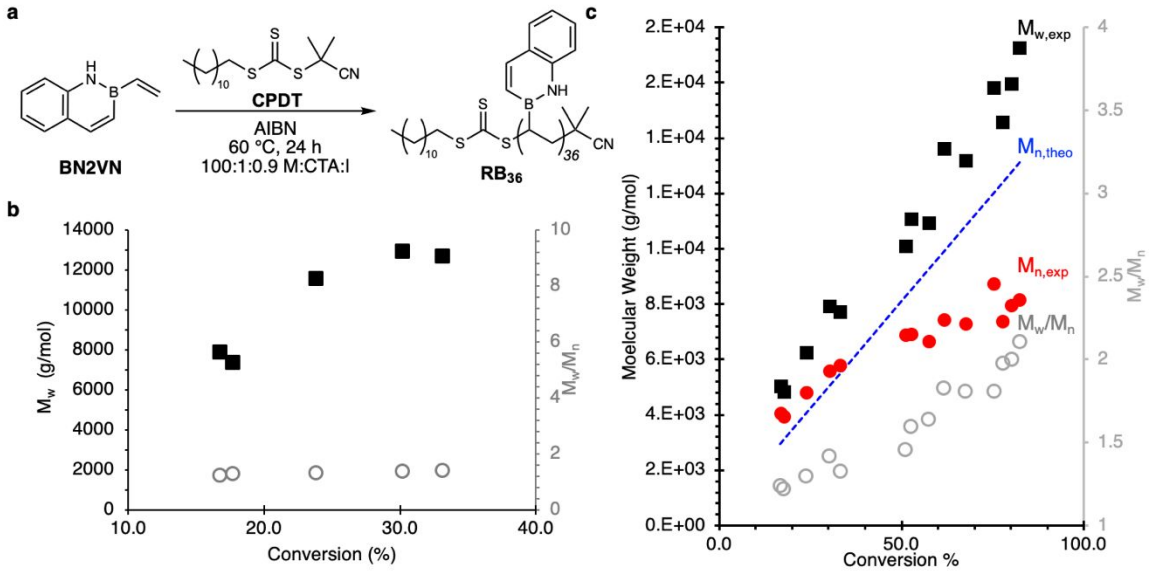

Figure 1. (a) RAFT polymerization of BN2VN. (b) Size exclusion chromatography (SEC) molecular weight data for PBN2VN runs up to 33.1% conversion displaying an increase in chain length with conversion with stable dispersity. (c) SEC weight data for PBN2VN runs through 82.1% conversion with loss of dispersity control at 52% conversion.

Between 10 and 30% conversion, we observed an increase in M_n and M_w (Figure 1b) with increasing conversion and consistently low dispersity (M_w/M_n = 1.24 to 1.40), Table 1). Good agreement was also found between the theoretical M_n and the experimental M_n determined via size exclusion chromatography (SEC, Table 1). These data are consistent with a controlled radical polymerization at lower conversion.

However, at higher conversions, molecular weight fidelity decreased (Figure 1c). The dispersity gradually increased to 2.0 (M_w/M_n =1.56 to 2.27). While the weight-average molar mass $M_{w,exp}$ continued to increase with the predicted $M_{n,theo}$, the increase in the number-average molar mass $M_{n,exp}$ deviated from predicted $M_{n,theo}$ above 30% conversion (Figure 1, Figure S2). These data were attributed to a significant extent of termination via disproportionation (e.g., formation of dead chains) even at low conversion.[4] This likely reflects the comparatively high concentration of initiator relative to CPDT; however, at lower concentrations of AIBN, sluggish reactivity was observed. While further investigation of RAFT conditions could address the poor molecular weight fidelity at high conversion, the focus of this manuscript was the synthesis of diblock copolymers and we therefore focused on characterization and chain extension of **RB_{36}**, a comparatively low molecular weight and low dispersity sample obtained from halting RAFT polymerization of BN2VN at ca. 30% conversion.

Table 1. Evolution of **RB** molecular weight characteristics with time.

	MALS[a]			**SEC**[b]			
% Conversion	M_n (g/mol)	M_w (g/mol)	M_w/M_n	M_n (g/mol)	M_w (g/mol)	M_w/M_n	$M_{n,theo}$ (g/mol)[c]
16.7	3940	5030	1.24	4,070	5,030	1.24	2,940
17.7	5720	4830	1.29	3,950	4,830	1.22	3,080
23.8	8770	6260	1.32	4,820	6,260	1.30	4,040

30.2	9360	7940	1.38	5,590	7,940	1.42	5,030
33.1	9130	7740	1.40	5,800	7,740	1.33	5,490
51.1	9880	10,100	1.56	6,900	10,100	1.46	8,270
52.6	12300	11,100	1.68	6,910	11,100	1.60	8,500
57.4	15100	10,900	1.70	6,660	10,900	1.64	9,240
61.6	10300	13,620	2.28	7,440	13,600	1.83	9,900
67.5	12000	13,200	2.12	7,290	13,200	1.81	10,800
75.4	19800	15,800	2.08	8,750	15,800	1.81	12,000
77.8	12400	14,600	1.96	7,380	14,600	1.98	12,400
80.2	10600	16,000	2.15	7,960	16,000	2.00	12,800
82.3	13000	17,300	2.27	8,160	17,300	2.11	13,100

[a] Determined via light scattering by LALS (1 mg mL^{-1}, THF, 10 μL, 0.35 mL min^{-1}, RT). [b] Determined relative to a polystyrene standard in refractive index mode of GPC (1 mg mL^{-1}, THF, 10 μL, 0.35 mL min^{-1}, RT). [c] Calculated according to the following equation, where X = conversion:

$$M_{n,theo} = X\frac{[BN2VN]}{[CPDT]}BN2VN_{MW} + CPDT_{MW}$$

Characterization of RB_{36}. An advantage of RAFT polymerization is well-defined end groups, which enable both post-polymerization functionalization and block copolymer synthesis.[40] We sought to characterize if the end groups of **RB_{36}** were consistent with CPDT termination (Figure 1a). Resonances consistent with the dodecyl chain of CPDT were identified by ^{1}H NMR spectroscopy (Figure S3). Thermogravimetric analysis (TGA) under nitrogen (Figure 2) provided additional evidence for a TTC end group. Two distinct phases of mass loss were identified. The first phase, beginning at ca. 200 °C, was assigned to end group thermolysis by comparison to TTC-terminated polystyrene.[41] The mass loss between 200 and 285 °C corresponded to 6.11% of the total mass, consistent with an expected value of 5.90% calculated from the M_n. The second phase of mass loss, between 300 and 450 °C, was assigned to depolymerization of **RB_{36}** to BN2VN monomer. While matrix-assisted laser desorption ionization (MALDI) mass spectrometry can be a powerful method for confirming end group structure in well-defined macromolecules, for BN2VN-based polymers, low signal was obtained suggesting challenges in ionization (Figure S4).

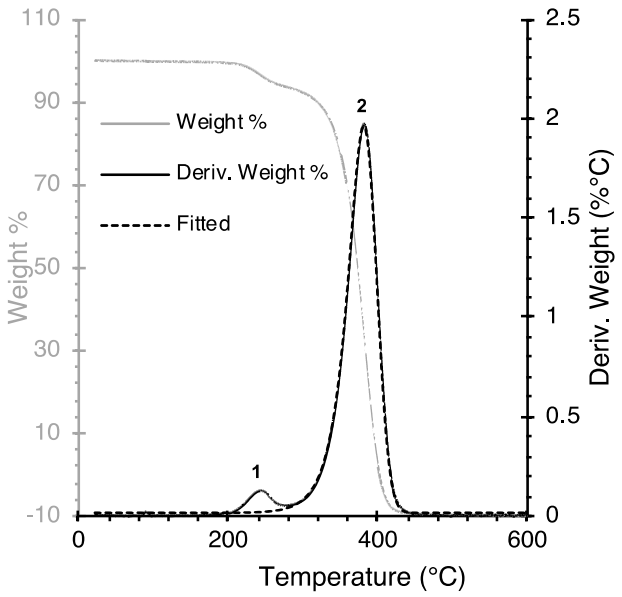

Figure 2. Overlay of TGA (weight % black, derivative weight % gray) and deconvoluted TGA curve (dashed) using Igor 8 multi-peak function with fitted ExpModGauss peak type shows two major degradation events (assigned 1, end-group and 2, PBN2VN block).

Chain Extension of RB_{36}. Having confirmed the presence of a TTC end group in **RB_{36}**, we attempted the synthesis of a styrene-BN2VN block copolymer **RB_{36}-*b*-RS** by chain extension under two different sets of conditions (AIBN, 70 °C or 120 °C, Figure 3a). Unfortunately, initiation of styrene polymerization from **RB_{36}** as the macro-CTA was unsuccessful. SEC analysis of a typical, successful block copolymer synthesis would show a monomodal elugram shifted to shorter retention time relative to the starting homopolymer block, which is interpreted as consistent with addition of a second block to the first.[42] In our hands, we observed bimodal elugrams by SEC (Figure 3b): a major peak was found at the same retention time as **RB_{36}**, while a new peak at higher molecular weight was also observed regardless of attempted chain extension conditions.

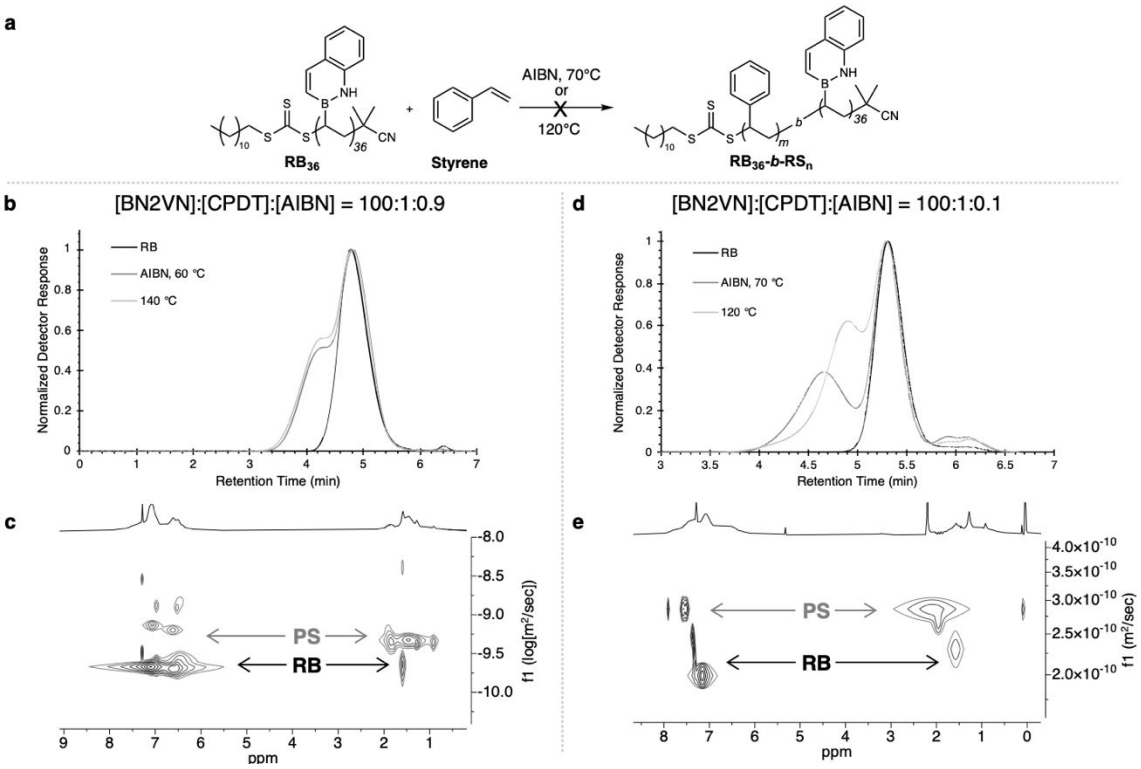

Figure 3. (a) Reaction conditions for attempted chain extension of RB. (b) GPC trace overlays (THF, 1.0 mg mL^{-1}, RT) for RB (black) and chain extension attempts with radical initiator AIBN (dark grey) and with thermally initiated conditions (light grey). (c) DOSY (400 MHz, $CDCl_3$) spectrum showing two macromolecules in solution from initiator chain-extension attempt of RB. (d) GPC trace overlays (THF, 1.0 mg mL^{-1}, RT) for RB (black) and chain extension attempts with radical initiator AIBN (dark grey) and with thermally initiated conditions (light grey). (e) DOSY (400 MHz, $CDCl_3$) spectrum showing two macromolecules in solution macromolecules in solution from thermal chain-extension attempt of RB.

Add conditions

We suggest that the bimodal elugrams are more consistent with styrene homopolymerization, rather than formation of a diblock copolymer, although partial chain extension could be difficulty to rule out completely. Diffusion-oriented NMR spectroscopy (DOSY) supported the formation of a styrene homopolymer **PS**, as we observed two different cross peaks with different diffusion constants (Figure 3c, S5-S6). The styrene homopolymer could arise from free radical polymerization initiated by AIBN or via thermal autoinitiation.[43]

The results may reflect the relatively high reactivity of styrene compared to BN2VN. In prior work, we showed via DFT calculated bond dissociation energies (BDEs) that the BN naphthalene ring of BN2VN stabilizes an adjacent radical less well than the simple benzene ring by about 4 kcal mol^{-1} (ethylbenzene BDE = 83.0; ethyl BN naphthalene BDE = 87.3 kcal mol^{-1}).[30] While a relatively small difference, these effects were found to result in measurable differences in chain transfer to toluene[28] and could account for a preference for styrene autopolymerization rather than diblock copolymer formation. Use of RB synthesized under more typical [CTA]/[initiator] conditions ([BN2VN]/[CPDT]/[AIBN] = 100:1.0:0.10 resulted in a similar mixture of homopolymers (Figure 3d-e), which suggests that the lack of chain extension does not reflect a high proportion of dead ends originating from a higher concentration of initiator.

Chain Extension of RS_{48}. A simple solution to address this reactivity challenge was to invert the order of block syntheses. The CPDT-terminated polystyrene **RS_{48}** was synthesized in bulk with AIBN (M:CPDT:I 100:1:0.1) at 70°C for 24 hours at 75% conversion to yield a macro-RAFT agent with an M_n of 5340, M_w of 6520 and M_w/M_n of 1.22. Chain extension of **RS_{48}** was achieved with BN2VN and AIBN (M:I 100:0.9, Figure 4a) at varying reaction times (Figure S7) and monomer feed ratios (Figure S8). This allowed us to tailor the length of the BN2VN block from a number-average degree of polymerization of 17 to 38, based on MALS (Table 2).

Table 2. Molecular weight characteristics of different **RS_{48}-b-RB_n** samples.

	MALS[a]				SEC[b]			
Polymer	M_w (g/mol)	M_w/M_n	M_n (g/mol)	DP	M_w (g/mol)	M_w/M_n	M_n (g/mol)	DP
RS_{69}	9,930	1.32	7,530	69St	10,100	1.25	8,050	74BN
4:1 RS_{69}-*b*-RB_{17}	13,800	1.37	10,100	17BN	10,800	1.27	8,470	3BN
2:1 RS_{69}-*b*-RB_{25}	16,500	1.44	11,400	25BN	11,600	1.28	9,080	7BN
1:1 RS_{69}-*b*-RB_{38}	26,500	1.96	13,500	38BN	16,700	1.52	11,000	19BN

[a] Determined via light scattering by LALS (1 mg mL^{-1}, THF, 10 μL, 0.35 mL min^{-1}, RT). [b] Determined relative to a polystyrene standard in refractive index mode of GPC (1 mg mL^{-1}, THF, 10 μL, 0.35 mL min^{-1}, RT).

Unlike our previous attempts at chain extensions, we now observed a single, monomodal elugram shifted to shorter retention times, consistent with an increase in hydrodynamic radius due to the presence of a second block (Figure 4b). As also observed in BN2VN homopolymerization, worsening control over dispersity was found at longer reaction times and higher BN2VN feed (M_w/M_n =1.37-1.96).

In addition to the unimodal SEC curve, significant supporting evidence for a single block copolymer was found. ^{1}H NMR spectroscopy indicated retention of the CPDT end-group (peaks at 0.90 ppm, 1.28 ppm, and 3.26 ppm, Figure 4a). In addition, resonances consistent with the BN naphthalene side chain were observed in the aromatic region. While these resonances could also be consistent with a blend of homopolymers, the observation of one major diffusion coefficient by DOSY NMR suggested a single copolymer (Figure S9). TGA analysis showed three phases of mass loss, compared to the two observed for the **RB_{36}** homopolymer, which were assigned to end group thermolysis, styrene block decomposition, and PBN2VN block decomposition (Figure 4c).

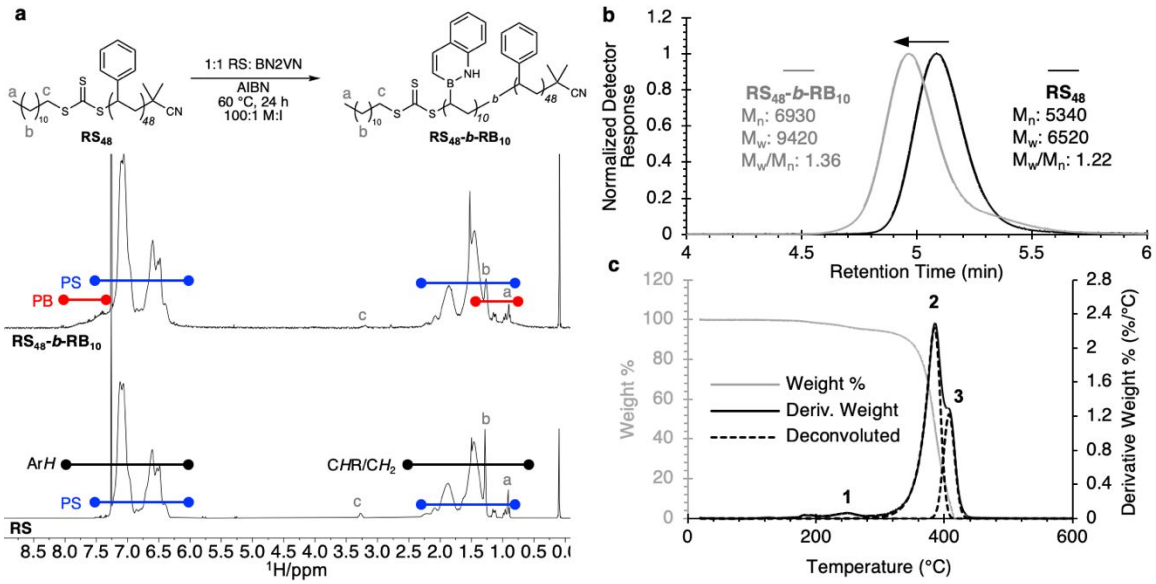

Figure 4. (a) The chain extension of **RS$_{48}$** to **RS$_{48}$-*b*-RB$_{10}$** was successful with retention of the trithiocarbonate end group by ^{1}H NMR. (b) Unimodal GPC traces show a decrease in retention time. (c) Overlay of TGA (weight % b) and deconvoluted TGA curves (dashed) using Igor 8 multi-peak function with fitted ExpModGauss peak type (gray, dashed) shows three major pyrolysis events (assigned end-group, PS block, and PBN2VN block).

Oxidation of RS-*b*-RB. With the styrene-BN2VN block copolymer **RS$_{48}$-*b*-RB$_{10}$** in hand, oxidative transformation of the BN2VN block to VA was explored. We chose to employ alkaline hydrogen peroxide (H_2O_2/NaOH, Figure 5a), which was previously found to provide conversions up to 99% in styrene-BN2VN statistical copolymers.[44]

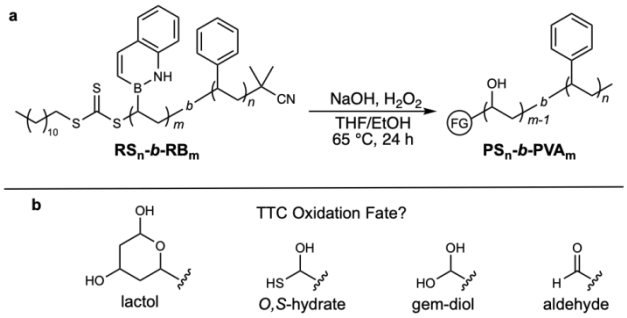

Figure 5. (a) Post-polymerization oxidation to form PS-*b*-PVA BCPs through the B-C functionalization of the PBN2VN block. (b) Potential end-group fates for the oxidation of a trithiocarbonate.

Oxidation had a significant effect on the physical properties of the samples. While **RS$_{48}$** and **RS-*b*-RB** are yellow due to the absorbance of the TTC end group and/or BN naphthalene side chain, the oxidized samples were white (Figure 6). Most of the PS-*b*-PVA copolymers were insoluble in THF, $CDCl_3$, and DMSO-d_6, in contrast to the good solubility of the precursors **RS** and **RS-*b*-RB**.

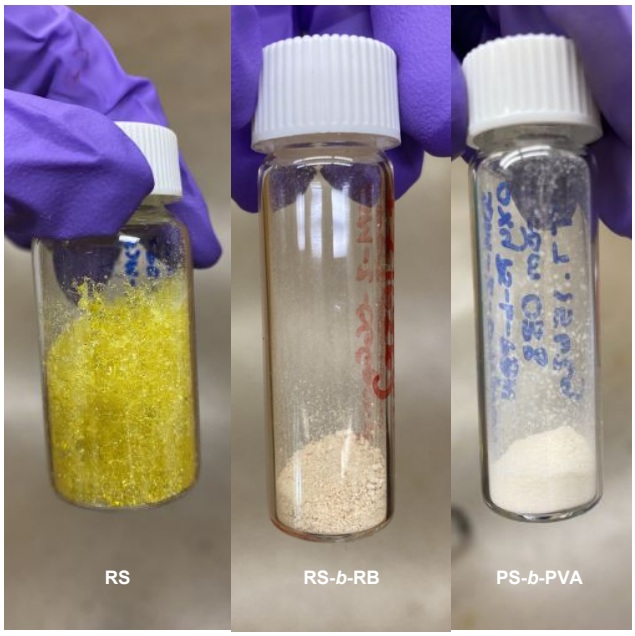

Figure 6. Physical appearance of pure RS, RS-*b*-RB, and PS-*b*-PVA.

Characterization of PS-*b*-PVA. Characterization proved to be difficult due to low solubility in NMR and SEC solvents for PS-*b*-PVA derived from polymers with longer BN2VN blocks (Figure S10). However, the block copolymers derived from oxidation of **PS_{48}-*b*-PB_{10}** and **PS_{48}-*b*-PB_{16}** proved soluble in THF and $CDCl_3$ and characterization data for these samples are described below.

By SEC, a dramatic decrease in absorbance at 310 nm for SEC UV-Vis mode was observed (Figure 7a). This is the wavelength where both the TTC end group and the BN naphthalene side chain are known to absorb, supporting a successful cleavage of the sidechains, as well as modification of the end groups (Figure S11). ATR-IR spectra show the appearance of a broad alcohol peak post-oxidation at 3377 cm^{-1} and disappearance of the sharper NH stretching frequency, indicating successful conversion of the BN naphthalene block to vinyl alcohol (Figure 7b). In RI mode and with multi-angle light scattering, molecular weight characteristics for oxidized **RS_{48}-*b*-RB_{10}** could be obtained (Table 3). We observe non-classical SEC traces and molecular weight data (e.g., an apparent increase in M_w by MALS after oxidation), which we attributed to potential inter-chain hydrogen-bonding of the PVA block, known to result in anomalous elution behavior.[42]

Table 3. SEC molecular weight data for **RS**, **RS-*b*-RB**, and **PS-*b*-PVA** from MALS and SEC.

	MALS[a]				SEC[b]			
Polymer	M_w (g/mol)	M_w/M_n	M_n (g/mol)	DP[c]	M_w (g/mol)	M_w/M_n	M_n (g/mol)	DP[c]
RS_{48}	6,520	1.22	5,340	48St	5,700	1.15	4,950	44St
RS_{48}-*b*-RB_{10}	9,420	1.36	6,930	10BN	8,300	1.23	6,760	12BN
RS_{48}-*b*-RB_{16}	11,700	1.51	7,780	16BN	8,960	1.27	7,030	13BN
PS_{48}-*b*-PVA_{10}	34,400	2.16	15,900		7,050	1.30	5,420	
PS_{48}-*b*-PVA_{16}	80,800	3.41	23,700		13,800	1.97	7,000	

[a] Determined via light scattering by LALS (1 mg mL^{-1}, THF, 10 μL, 0.35 mL min^{-1}, RT). [b] Determined relative to a polystyrene standard in refractive index mode of GPC (1 mg mL^{-1}, THF, 10 μL, 0.35 mL min^{-1}, RT). [c] Calculated according to the following equation: $\boldsymbol{RS_{DP}} = \frac{(\boldsymbol{M_n} - \boldsymbol{CPDT_{MW}})}{\boldsymbol{Styrene_{MW}}}$ and $\boldsymbol{BCP_{DP}} = \frac{(\boldsymbol{M_n} - \boldsymbol{RS_{MW}})}{\boldsymbol{BN2VN_{MW}}}$

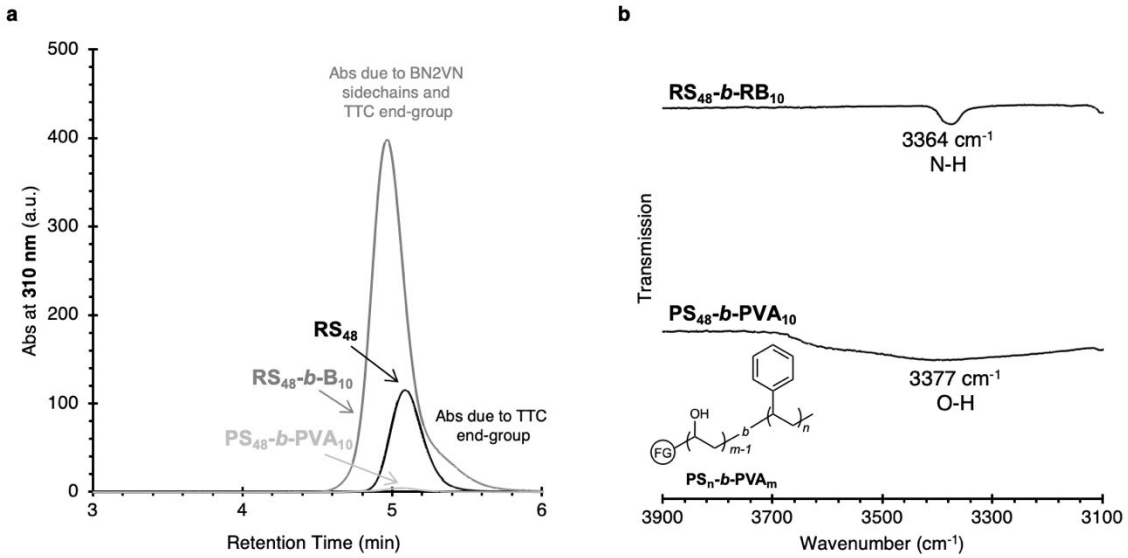

Figure 7. (a) SEC curve overlays at 310 nm absorbance detector mode (a UV handle for BN2VN and trithiocarbonate) for RS (black), RS-*b*-RB (dark gray) and PS-*b*-PVA (light gray). (b) ATR-FTIR overlay of chain extended BCP RS-*b*-RB, and functionalized PS-*b*-PVA showing the appearance of a broad OH stretch peak.

Further support for the C–B to C–OH transformation was obtained from solid-state ^{13}C CP MAS NMR spectra, which could be employed for all samples, regardless of solubility. Figure 8 compares the ^{13}C CP MAS spectra of the styrene and vinyl alcohol homopolymers to the block copolymers. After chain extension with BN2VN, a comparison of **RS$_{48}$** and **RS$_{48}$-*b*-RB$_{119}$** reveals additional resonances in the aromatic region consistent with the BN naphthalene side chain. The overall broadening of ^{13}C peaks in **RS$_{48}$-*b*-RB$_{119}$** was attributed to quadrupolar relaxation of boron. After oxidation with H_2O_2/NaOH, the aromatic resonances assigned to BN naphthalene disappeared, while the styrenic resonances were maintained in three different block copolymers of different PVA block length. In addition, a ca. δ 70 resonance was observed that is consistent with the C–OH methine resonance of PVA (Figure 8). The intensity of this resonance increased with the length of the starting BN2VN block.

We hypothesized that during the aqueous oxidation conditions, the TTC end group would be converted to an alcohol, as has been previously described for dithiobenzoate-capped polyacrylates.[45] To test this hypothesis, we subjected **RS$_{48}$** to the oxidation conditions and observed by ^{13}C CPMAS a sharp *C*-OH peak at 68 ppm indicative of transformation of the TTC end group to an alcohol (Figure S12). Given the head-to-tail polymerization expected for a bulky side chain, oxidative conversion of **RS$_{48}$-*b*-RB** to **PS-*b*-PVA** would result in an end group carbon with the oxidation state of an aldehyde due to transformation of both the C–B and C–S bonds to C–O bonds (Figure 5b). The equilibrium between an aldehyde and a hydrate (e.g., gem-diol) is close to 1, while the equilibrium between a lactol and a hydroxy-aldehyde favors the lactol for 5- and 6-membered rings. This suggests that spectroscopic signatures of an aldehyde end group should not be expected and indeed were not observed by FTIR or NMR spectroscopy. Strong

evidence for the gem-diol or lactol were not found, however, these may be in equilibrium with each other.

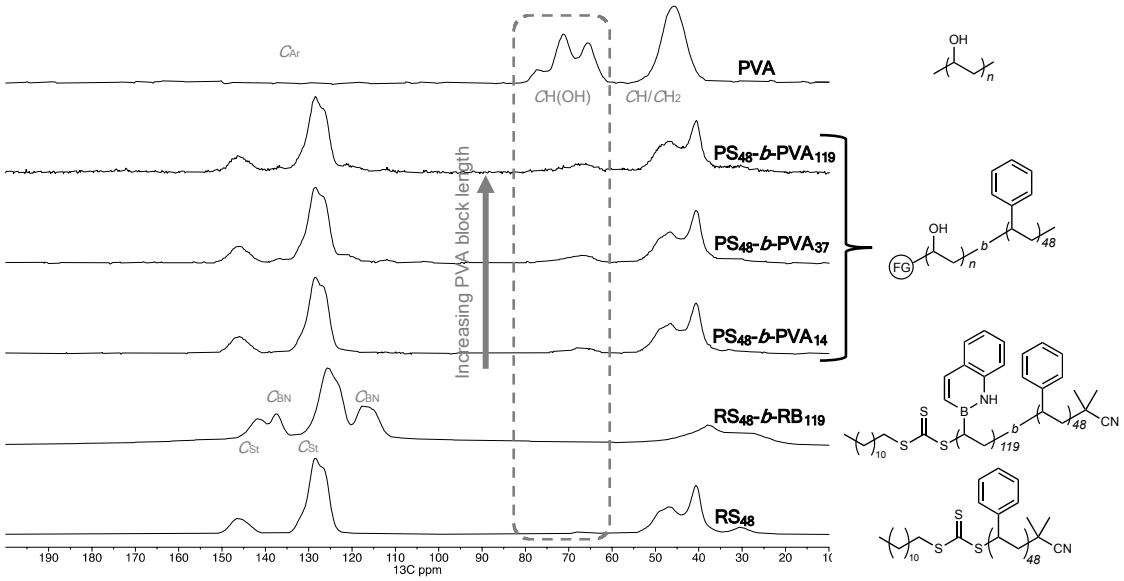

Figure 8. Solid state ^{13}C NMR overlay of **RS**, **RS-*b*-RB**, **PS-*b*-PVA** with varying precursor RB block lengths, and commercially available PVA. C-OH region is highlighted in grey.

As an alternative to NMR spectroscopy, we investigated MALDI. The MALDI data for the macro-CTA $\mathbf{RS_{48}}$ are shown in Figure 9. The mass spectrum shows a M_n of 5740 g mol^{-1}, which corresponds very well with the M_n of 5738 g mol^{-1} as determined by SEC. Unfortunately, in the copolymers containing BN2VN or VA blocks, a combination of low solubility in the deposition solvent and poor ionizability led to a much lower signal to noise ratio than for $\mathbf{RS_{48}}$. However, peak intervals corresponding to coincident monomeric subunits of St (104.0 m/z) and BN2VN (154.8 m/z) as well as St and VA (44.4 m/z) provided further evidence of successful chain extension and oxidation. It is possible to determine the length of each monomer block contributing to the series of copolymer peaks, as they show strong agreement with the expected adduct m/z values for RS, RS-*b*-RB, and PS-*b*-PVA (Figure S4). In doing so, it is evident that only PS-*b*-PVA chains with one VA segment were appreciably detectable via MALDI-TOF, likely due to the poor solubility characteristics of those containing longer PVA blocks.

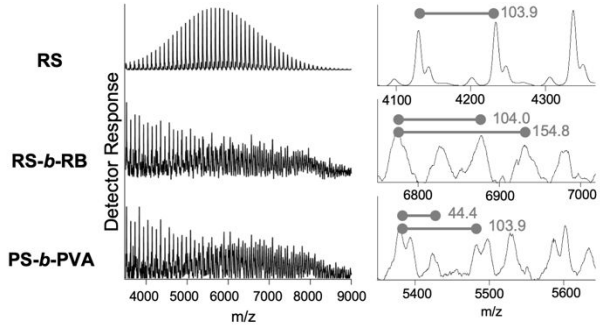

Figure 9. MALDI of RS_{48}, RS_{48}-*b*-RB_{10}, and PS_{48}-*b*-PVA_{10} BCPs. BN2VN MW: 155.09 g mol^{-1}, Styrene MW: 104.15 g mol^{-1}, VA MW: 44.02 g mol^{-1}.

Conclusions

A new method to achieve polystyrene-*block*-polyvinyl alcohol copolymers with tailorable PVA block lengths was introduced. RAFT polymerization of BN2VN with CPDT yielded macro-RAFT agents, but chain-extension with styrene was not observed, despite strong evidence of trithiocarbonate (TTC) termination (^{1}H NMR, TGA). Instead, chain extension of a styrenic macro-RAFT agent with BN2VN was successful and through variation of the reaction conditions we synthesized four distinct styrene-BN2VN block copolymers where the BN2VN block length varied from 10 to 40 degrees of polymerization. We demonstrated that aqueous oxidation transformed the C–B side chain to C–OH, while also cleaving the TTC end group. Solid-state NMR, ATR-IR, SEC spectra and thermogravimetric analysis support the conversion of the PBN2VN blocks to PVA. This work expands the utility of the BN2VN monomer; we foresee broader use of the living polymerization of BN2VN with various RAFT agents and B-C functionalizations.

Acknowledgements

This material is based upon work supported by the National Science Foundation under grant CHE-2304952. CPMAS spectroscopy was made possible through the National Science Foundation Major Research Instrumentation grant CHE-2018176. E. G. A. thanks Johns Hopkins University for the Provost's Undergraduate Research Award. We thank Prof. V. Sara Thoi, Dr. Rasha Anayah, and Mr. Ian Dillingham (JHU) for the use of thermogravimetric analysis and Ms. Randinu Pulukkody of Prof. E. Pentzer's group (Texas A&M) for MALDI support.

Notes and references

1 M. L. Hallensleben, R. Fuss and F. Mummy, in *Ullmann's Encyclopedia of Industrial Chemistry*, Wiley-VCH Verlag GmbH & Co. KGaA, Weinheim, Germany, 2015, pp. 1–23.
2 K. Matyjaszewski and J. Xia, *Chem. Rev.*, 2001, **101**, 2921–2990.
3 D. Benoit, V. Chaplinski, R. Braslau and C. J. Hawker, *J. Am. Chem. Soc.*, 1999, **121**, 3904–3920.
4 S. Perrier, *Macromolecules*, 2017, 50, 7433–7447.
5 G. Moad and D. H. Solomon, *The Chemistry of Radical Polymerization*, Elsevier Ltd, 2nd edn., 2006.
6 Y. Morishima and S. Nozakura, *J. Polym. Sci. Polym. Chem. Ed.*, 1976, **14**, 1277–1282.
7 S.-I. Nozakura, Y. Morishima and S. Murahashi, *J. Polym. Sci. Part A-1 Polym. Chem.*, 1972, **10**, 2853–2866.
8 D. Britton, F. Heatley and P. A. Lovell, *Macromolecules*, 1998, **31**, 2828–2837.
9 D. Mardare and K. Matyjaszewski, *Macromolecules*, 1994, **27**, 645–649.
10 E. Yoshida, *Colloid Polym. Sci.*, 2010, **288**, 73–78.
11 M. P. Shaver, M. E. Hanhan and M. R. Jones, *Chem. Commun.*, 2010, **46**, 2127–2129.
12 M. H. Stenzel, L. Cummins, G. E. Roberts, T. P. Davis, P. Vana and C. Barner-Kowollik, *Macromol. Chem. Phys.*, 2003, **204**, 1160–1168.
13 M. Wakioka, K. Y. Baek, T. Ando, M. Kamigaito and M. Sawamoto, *Macromolecules*, 2002, **35**, 330–333.
14 M. Destarac, D. Charmot, X. Franck and S. Z. Zard, *Macromol. Rapid Commun.*, 2000, **21**, 1035–1039.
15 M. C. Iovu and K. Matyjaszewski, *Macromolecules*, 2003, **36**, 9346–9354.
16 Y. Y. Tong, Y. Q. Dong, F. S. Du and Z. C. Li, *Macromolecules*, 2008, **41**, 7339–7346.
17 C. M. Liao, C. C. Hsu, F. S. Wang, B. B. Wayland and C. H. Peng, *Polym. Chem.*, 2013, **4**, 3098–3104.
18 C. Sinturel, F. S. Bates and M. A. Hillmyer, *ACS Macro Lett.*, 2015, **4**, 1044–1050.
19 H. G. Jeon and J. H. Youk, *Macromolecules*, 2010, **43**, 2184–2189.
20 A. Debuigne, J. R. Caille, N. Willet and R. Jérôme, *Macromolecules*, 2005, **38**, 9488–

9496.
21 Y. J. Chen, B. J. Wu, F. S. Wang, M. H. Chi, J. T. Chen and C. H. Peng, *Macromolecules*, 2015, **48**, 6832–6838.
22 O. Altintas, J. C. Speros, F. S. Bates and M. A. Hillmyer, *Polym. Chem.*, 2018, **9**, 4243–4250.
23 J. Muller, F. Marchandeau, B. Prelot, J. Zajac, J. J. Robin and S. Monge, *Polym. Chem.*, 2015, **6**, 3063–3073.
24 R. Nicolaÿ, Y. Kwak and K. Matyjaszewski, *Chem. Commun.*, 2008, 5336–5338.
25 M. Wang, X. Jiang, Y. Luo, L. Zhang, Z. Cheng and X. Zhu, *Polym. Chem.*, 2017, **8**, 5918–5923.
26 D. Kumar, S. A. Mohammad, M. M. Alam and S. Banerjee, *Polym. Chem.*, 2022, **13**, 517–526.
27 H. L. van de Wouw, J. Y. Lee, E. C. Awuyah and R. S. Klausen, *Angew. Chemie - Int. Ed.*, 2018, **57**, 1673–1677.
28 Y. Ji and R. S. Klausen, *J. Polym. Sci.*, 2021, **59**, 2521–2529.
29 Y. Ji, T. Zhou, H. L. Van De Wouw and R. S. Klausen, *Macromolecules*, 2020, **53**, 249–255.
30 H. L. van de Wouw, E. C. Awuyah, J. I. Baris and R. S. Klausen, *Macromolecules*, 2018, **51**, 6359–6368.
31 H. L. van de Wouw, J. Y. Lee and R. S. Klausen, *Chem. Commun.*, 2017, **53**, 7262–7265.
32 S. N. Mendis, T. Zhou and R. S. Klausen, *Macromolecules*, 2018, **51**, 6859–6864.
33 J. Huang, Y. Jiang, Z. Zhang, S. Li and D. Cui, *Macromol. Rapid Commun.*, 2020, **41**, 2000038.
34 F. R. Mayo, C. Walling, F. M. Lewis and W. F. Hulse, *J. Am. Chem. Soc.*, 1948, **70**, 1523–1525.
35 A. Suzuki, *Angew. Chemie Int. Ed.*, 2011, **50**, 6722–6737.
36 S. N. Mlynarski, A. S. Karns and J. P. Morken, *J. Am. Chem. Soc.*, 2012, **134**, 16449–16451.
37 T. Nishikawa and M. Ouchi, *Angew. Chemie - Int. Ed.*, 2019, **58**, 12435–12439.
38 T. Kanazawa, T. Nishikawa and M. Ouchi, *Polym. J.*, 2021, **53**, 1167–1174.
39 H. Makino, T. Nishikawa and M. Ouchi, *Chem. Commun.*, 2021, **57**, 7410–7413.
40 H. Willcock and R. K. O'Reilly, *Polym. Chem.*, 2010, 1, 149–157.
41 A. Postma, T. P. Davis, G. Moad and M. S. O'Shea, *Macromolecules*, 2005, **38**, 5371–5374.
42 K. Philipps, T. Junkers and J. J. Michels, *Polym. Chem.*, 2021, **12**, 2522–2531.
43 K. S. Khuong, W. H. Jones, W. A. Pryor and K. N. Houk, *J. Am. Chem. Soc.*, 2005, **127**, 1265–1277.
44 Y. Ji, J. Catazaro, Q. Jiang, S. J. Melvin, J. Jiang and R. S. Klausen, *Macromolecules*, 2022, **55**, 7032–7038.
45 C. P. Jesson, C. M. Pearce, H. Simon, A. Werner, V. J. Cunningham, J. R. Lovett, M. J. Smallridge, N. J. Warren and S. P. Armes, *Macromolecules*, 2017, **50**, 182–191.